CREATING A CELL-FREE ASSAY TO ASSESS THE BINDING AFFINITY OF PATIENT VARIANTS IN THE BRCA1-PALB2 INTERFACE

by

CHRISTINE ANN HURD

Artium Baccalaureus, 2013
Harvard University
Cambridge, Massachusetts

Submitted to the Graduate Faculty of the
College of Science and Engineering
Texas Christian University
in partial fulfillment of the requirements
for the degree of

Master of Science

May 2020

ACKNOWLEDGMENTS

I am eternally grateful for Dr. Mikaela Stewart for her intellect, patience, dedication, wisdom and her constant application of those qualities to The Work.

I deeply appreciate the time and feedback given by the members of my committee: Dr. Giri Akkaraju and Dr. Meredith Curtis.

I thank my mother, Doris Hurd, and my sister, Catherine Hurd, for their high spirits in stressful times.

TABLE OF CONTENTS

LIST OF FIGURES

LIST OF TABLES

I. INTRODUCTION

According to the American Cancer Society, It is estimated that there will be 276,100 new cases of breast cancer diagnosed in the United States in 2020. [2] Of these breast cancer cases, approximately 20% of patients will have inherited *BRCA1* or *BRCA2* mutations. [3] The lifetime breast cancer risk for a woman with a deleterious *BRCA1* mutation is 87% and lifetime ovarian cancer rate is 44%. [4] However, if a patient knows that she has a deleterious germline mutation, this lends the option of risk-reducing surgery: either an oophorectomy, which has been shown to reduce risk of ovarian cancer by approximately 90% or a bilateral mastectomy, which reduces risk of breast cancer by approximately 50%. [5] Unfortunately, the nature of every germline *BRCA1*-family mutation—whether beneficial, neutral, or deleterious—is vastly unknown; these variants are classified as Variants of Unknown Significance or VUS **(Figure 1)**.

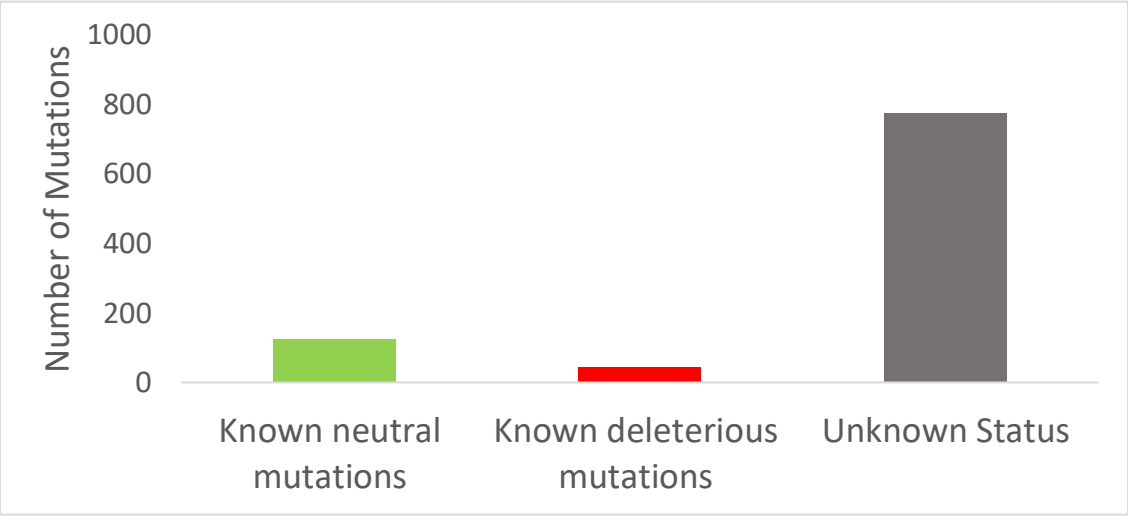

Figure 1: Characterization of missense mutations in *BRCA1*. Shown above are the number of neutral, deleterious and VUS in *BRCA1*. Source: *BRCA1*share.

A significant number of VUS are located in a region of BRCA1 that is used to interact with PALB2 (Partner and Localizer of BRCA2). BRCA1 and PALB2 are both tumor-suppressing proteins that are required for double-stranded break repair via homologous recombination. [1] When double-stranded break repair functionality is lost, then mutations rapidly accumulate, genomic instability is incurred, and a cell's likelihood to become cancerous is raised significantly. One way that a loss of function can occur is if two proteins in the DNA repair complex lose their ability to bind to each other. Through pull-down experiments, it has been shown that the 5-91 amino acid region of PALB2 and the 1393-1476 amino acid region of BRCA1 are necessary for PALB2-BRCA1 complex formation. [6] An NMR structure currently exists for PALB2 in this N-terminal region, and it was found that the N-terminal region of PALB2 is a leucine zipper, homodimeric anti-parallel alpha helix. [7] Functionally, PALB2 and BRCA1 bind as a heterodimer under conditions of DNA damage; otherwise, PALB2 primarily associates with itself as this alpha-helical homodimer. It is currently theorized that BRCA1, which is known to be intrinsically disordered in the binding region, folds into an alpha helix in order to bind to PALB2. [1, 8] However, with the exception of a proof-of-concept non-natural mutation made in the PALB2 homodimer interface (L24A), there have not been structural studies of natural variants and their effect on folding and function. [7]

Current methods used to categorize VUS in BRCA1 and PALB2 and their limitations

There are several methods that have been applied to predicting whether a mutation in BRCA1 or PALB2 is deleterious. Methods that have been used so far to study the effects of mutation on this interaction's interface are summarized for quick comparison in **Table 1**. In terms of clinical application, the formation of a pedigree of family members of a patient with a given natural variant provides the most direct connection between genotype and phenotype. Shortly after

PALB2 was identified as a binding partner of BRCA2, pedigrees were constructed of breast cancer patients who did not have mutations in *BRCA1* or *BRCA2*—and it was found that certain *PALB2* mutations conferred a modest increased risk of breast cancer. [9] [10] Genome-wide association studies (GWAS), which use large swaths of patient genomic data to draw associations between single nucleotide polymorphisms (SNPs) and health outcomes. SNPs are differences at one locus in one base pair of DNA that have been identified as having two separate populations. For example, one base pair in a given gene might be "A" in 95% of the population and "C" in 5% of the population. If patients who have "C" have a much higher propensity for lung cancer, for example, then that position might be in a gene related to growth signaling in lung tissue or be related structurally to a gene that is. GWAS has been applied to breast cancer patients, and several dozen significant single nucleotide polymorphisms (SNPs) have been identified; however, since most of the mutations in PALB2 are not high penetrance, it is unsurprising that GWAS does not often flag PALB2-related SNPs. [11] However, there have been several gene association analyses that have identified PALB2-related SNPs in Asian breast cancer patient populations. [12] [13] In addition to collating patient information with genotypes, we can also gain information about how a protein works through functional assaying. By using wild-type and mutated versions of a target protein such as PALB2 and assessing various biochemical outcomes from binding to genome stability, we can see how a certain mutation might affect cancer-risk. Mammalian two-hybrid assays have been a popular choice for assessing PALB2 variants and have found reduced binding activity to BRCA1 for the PALB2 VUS, Y28C. [14] [15] Rad51 foci formation showed moderate decreases in cells with the PALB2 VUS P8L and Y28C, and PARPi sensitivity assays also marked P8L as a more detrimental variant. [15] On the other side of the interface and the broader side of studying mutations, saturation genome

editing has been performed on *BRCA1*. [16] However, it is important to keep in mind that these assays give an all or none perspective; even if a mutation does not appear to abolish activity in one of these functional assays, it can, over a lifetime, lead to an increased risk of cancer if there is an undetectable decrease in activity.

Table 1: A survey of methods that have been used to assess the effect of mutations on the BRCA1-PALB2 interface

Functional Assays			
Method Name	Description	Application	Challenges
Mammalian two-hybrid assay	Hybrid construct is made; if two proteins bind, then expression of reporter gene increases	Full-length proteins can be used; Has been applied to PALB2 VUS in BRCA1-binding region [14, 15]	Cells are used, which are difficult to cultivate
Saturation Genome Editing (SGE)	Every codon is mutated using Crispr/Cas9; functionality is assessed by cell survival after a loss of heterozygosity	Full coverage; has been applied to 96.5% of BRCA1 gene [16]	Not replicating actual patient mutations
Olaparib Sensitivity	PARP1 inhibitors greatly decrease cell survival if HR is compromised; thus can report on HR efficiency	Reporting if DSB repair is compromised; has been used for PALB2 VUS in BRCA1-binding region [14]	Human cells are used, which can be difficult to cultivate; for some variants, residual HR activity compensated in the cell
Rad51 Foci	If BRCA1/PALB2 interface is uncompromised, Rad51 will be recruited to DNA damage and can be measured with immunofluorescence.	Full length proteins are used; reporting on response to DNA damage; has been used to assess PALB2 VUS in BRCA1-binding region [14, 15]	Human cells are used, which are difficult to cultivate

Table 1 Cont.			
Genetic Methods			
GWAS	Large populations are sequenced and compared with phenotypic data	Has been used to identify high penetrance mutations, especially in BRCA1	Mutations can be in linkage disequilibrium Can miss VUS that are not widespread that don't have very high penetrance
Segregation Analysis	Personalized method that uses familial history and genotype to assess whether a patient's mutation has resulted in cancer through generations	Personalized specifically to mutation; early-onset breast cancer is distinguishable [10]	Requires many living female family members on one side of a family and is resource intensive
Other Methods			
In silico prediction	Computer software is used to predict if two proteins will bind	No wet lab work necessary, fast processing; has been applied to PALB2 VUS [15]	Different programs can predict opposite models for the same variant; unreliable

The development of a quantitative in vitro model for assessing VUS in the BRCA1-PALB2 binding interface

While there has recently been a surge in measuring the effects of PALB2 VUS using various functional assays, there has been less focus on the BRCA1 side of the interface in the PALB2-binding region. There also has not been, to our knowledge, the development of a cell-free functional assay to assess the effect of a mutation in PALB2 or BRCA1 on their binding interface. While many of these methods rely on human cell culture, an *in vitro* system using constructs grown in *E. coli* lends itself to better quantification of how much protein is present and thus gives us options of highly quantifiable methods to assess binding affinity such as

isothermal titration calorimetry (ITC). Since the binding region of each of these proteins is limited to 50-100 amino acids in length, we can also use truncated constructs and nuclear magnetic resonance (NMR) to observe the binding interface in either of the two binding partners to gain insight into the molecular details of binding that cannot be obtained from cell-based assays. While X-ray crystallography has been used successfully for other domains of both proteins such as the WD40 domain of PALB2 and the BRCT domain of BRCA1, the PALB2-binding region of BRCA1 is intrinsically disordered and therefore resistant to crystallization. Just as *ex vivo* methods have disadvantages, *in vitro* methods can come with challenges as well. For example, like many DNA repair proteins, both BRCA1 and PALB2 also undergo post-translational modification under conditions of DNA damage via the activity of ATM/ATR kinase: BRCA1 undergoes activating phosphorylation at three separate serine residues in its PALB2-binding region, and PALB2 undergoes one activating phosphorylation event (at Ser 59) and one deactivating phosphorylation event in its BRCA1 binding region (at Ser 64). [17] [18] Because our method uses *E. coli* cells, we lose the natural ability of a human cell to phosphorylate these sites using endogenous ATM/ATR kinase. We overcome this challenge using mutations that replace the phosphorylated amino acid with a charged amino acid to mimic phosphorylation at this position. This technique has been shown to recreate phosphorylation *in vitro* and *in vivo* for many systems.[19-21] Therefore, part of this project has been to also test constructs that have been phosphomimicked to see if we can observe structural or functional changes induced by post-translational modification.

Our aims

While there are several assays that have been used to assess various functions enacted by a successful PALB2/BRCA1 binding event, including homologous recombination assays and two-

mammalian hybrid assays, there is not an *in vitro* biochemical method to quickly assess binding affinity at this interface. Here I present methods to measure the folding and function of the BRCA1/PALB2 interaction using nuclear magnetic resonance (NMR), circular dichroism (CD), and isothermal titration calorimetry (ITC) to qualify and quantify the effects of natural variants and phosphorylation on the strengthening or weakening of this interaction.

II. RESULTS

Constructing an *in vitro* model to predict deleterious mutations in the BRCA1-PALB2 binding interface

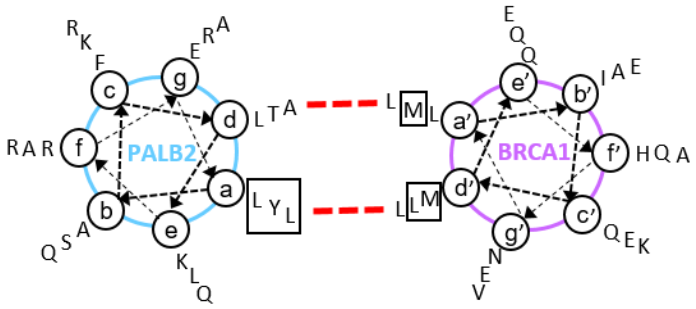

Figure 2) PALB2 and BRCA1 are predicted to form a heptad coiled-coil heterodimer. PALB2 naturally exists as an alpha helical homodimer, and intrinsically disordered BRCA1 is predicted to fold into a helix upon binding with PALB2. [1]

Our first goal was to investigate the BRCA1-PALB2 interface in order to predict which residues participate in binding and thus which would be more likely candidates for being deleterious mutations. Since BRCA1 and PALB2 have been previously predicted to form an alpha helical coiled-coil structure, our first goal was to test this hypothesis using two methods that can give information about a peptide's secondary structure: nuclear magnetic resonance (NMR) and circular dichroism (CD). [1] If BRCA1 and PALB2 form an alpha helical coiled-coil, then it would indicate that residues predicted to be in that interface would be more likely to be deleterious mutations (shown in red dotted lines in Figure 2). In order to investigate the structure, we created truncated protein constructs of both BRCA1 and PALB2 that represented the different phosphorylation states of each protein. Since the PALB2-binding region of BRCA1 is known to be phosphorylated at three of its serine residues upon conditions of DNA damage, we created a phosphomimetic BRCA1 construct using site-directed mutagenesis. Serine at the three sites was replaced with glutamic acid in order to simulate the negative charges conferred by kinases during phosphorylation events. In the following experiments, the non-phosphorylated and phosphomimetic constructs are referred to as BRCA1 0P and BRCA1 3P respectively. The BRCA1-binding region of PALB2 also has one serine phosphorylated upon DNA damage (Ser

59) and one serine phosphorylated in normal, non-DNA damage conditions (Ser 64). Therefore, we also created phosphomimetic PALB2 constructs that replicated these states, S59E and S64E respectively. We also used a more truncated construct of PALB2 (amino acids 1-56) meant to include only the coiled-coil predicted region that omitted the phosphorylated amino acids.

NMR is the first experimental method we used to glean information regarding the molecular details of the interaction interface and the structures of the two proteins. Since the PALB2-binding region of BRCA1 is known to be intrinsically disordered and relatively short in length, NMR is an appropriate method to confirm if a given BRCA1 construct and PALB2 construct bind *in vitro*. NMR can also show binding events that result in oligomerization as well as give structural information about a binding interface. Examples of these structural insights include whether or not a peptide is folding into a secondary structure upon binding or which amino acids are located in the binding interface. In **Figure 3**, we show that we can detect binding from both sides of the BRCA1 and PALB2 interface. In these NMR spectra, each of the circular target-shaped peaks reflects the chemical environment of one nitrogen-hydrogen bond of the labelled protein (either ^{15}N PALB2 in **3a** or ^{15}N BRCA1 in **3b**). NMR-viable proteins are created by growing our protein constructs with *E. coli* in the presence of isotopically-labelled ammonium chloride ($^{15}NH_4Cl$) as the only source of nitrogen. By adding NMR invisible proteins (grown with naturally abundant isotopes of ammonium chloride) we can see how the chemical environment of the labelled construct is changed when it interacts with an unlabeled protein. If there is a binding event, we can expect a shift in the location of whichever peaks of the labelled protein are interacting with the unlabeled protein. In **Figure 3**, peak shifts are marked with black arrows, showing that we can observe binding from both the PALB2 and BRCA1 sides of the interaction. We also see that BRCA1 does not fold upon binding (**Figure 3c**) or fold in response

to phosphomimetic mutations (**Figure 3d**). This is evident by the fact that the peaks corresponding to each backbone nitrogen-hydrogen pair do not spread out over the ^{1}H axis. As the PALB2-binding region of BRCA1 is intrinsically disordered, each nitrogen-hydrogen pair should be surrounded by water and buffer and thus have a relatively similar chemical environment. If BRCA1 were to fold into an alpha helix upon interaction with PALB2, these amides would be involved in hydrogen bonds significantly altering their chemical environment and dispersing the peaks centered around 8.0-8.5 ppm, and we have not observed that in repeated experiments.

CD was used to confirm that BRCA1 did not form an alpha helix upon binding with PALB2. Since the PALB2-binding region of BRCA1 is intrinsically disordered, any experimental method that indicated BRCA1 folds into an alpha helix upon titration with PALB2 would inform on the molecular details of the binding interface. CD is an experimental method that can predict secondary structure composition by passing circularly polarized light at different wavelengths through a protein of interest. Alpha helices, beta sheets, and intrinsically disordered secondary structures all form distinct characteristic curves. We can use this method to observe if either of our BRCA1 constructs fold into an alpha helix upon binding with PALB2. If a protein is completely alpha helical in nature, we can expect dips in the mean residual ellipticity (MRE) at 205-210nm and 220-225nm; if a protein is disordered, we can expect a rise in MRE from 200-220nm from negative to crossing the x-axis at ~210nm.

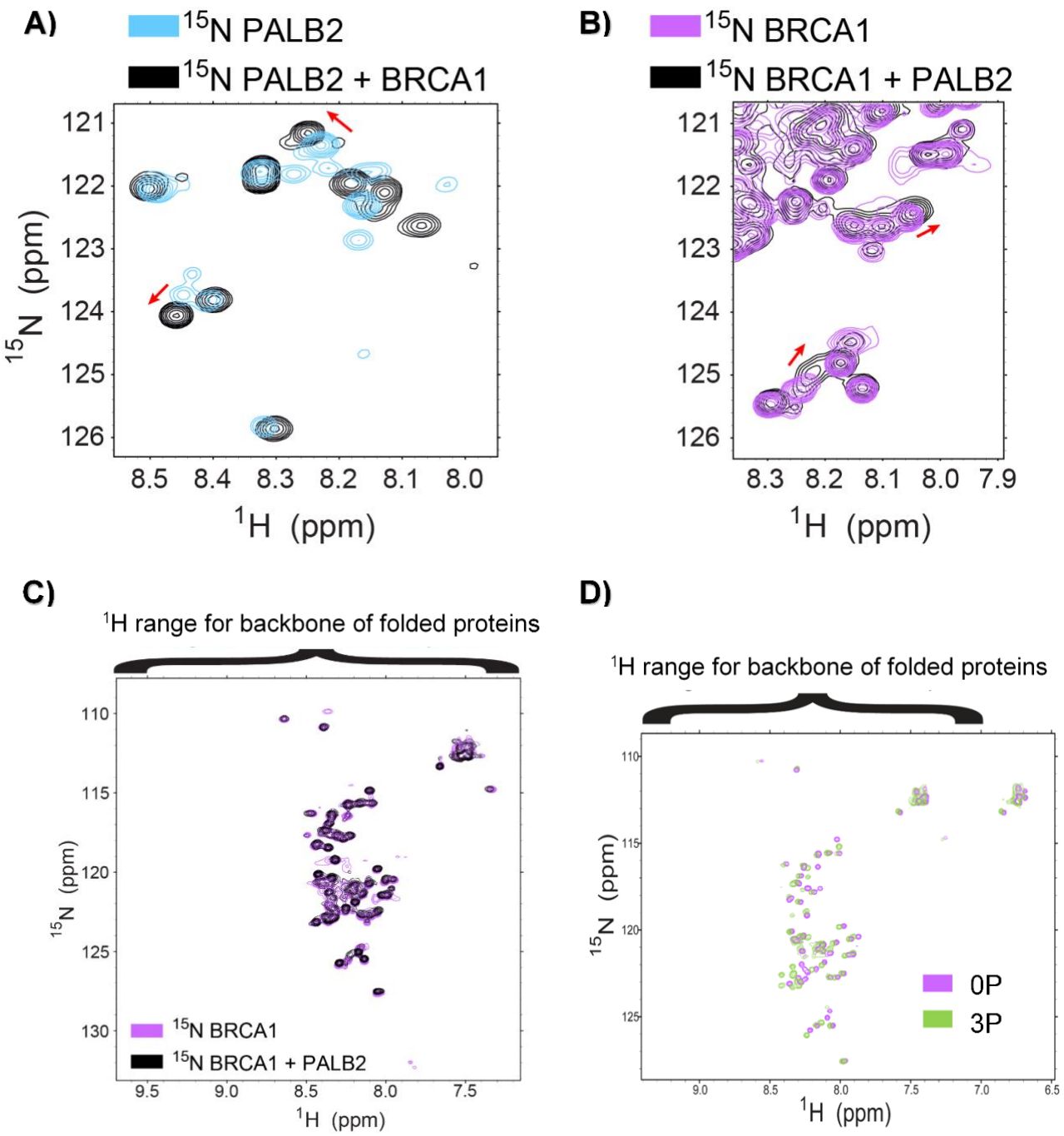

Figure 3) BRCA1 constructs bind to PALB2 constructs in vitro without folding into an alpha helix upon binding. A) ^{15}N PALB2 1-56 was titrated with naturally abundant (NA) BRCA1 1362-1481 construct. B) ^{15}N 0P BRCA1 1377-1467 was titrated with NA PALB2 1-93. C) A larger portion of the spectrum from 2b is shown relative to the range of ^{1}H ppm expected for folding proteins. D) Comparison of 0P and 3P BRCA1 spectra showing that both constructs are intrinsically disordered and similar to each other. Collection criteria for these experiments is detailed in the Methods Section.

In **Figure 4** we have reported that both 0P BRCA1 and 3P BRCA1 alone (green and pink curves respectively) are confirmed to be intrinsically disordered and do not appear to fold into an alpha helix upon titration with PALB2 constructs. If either 0P BRCA1 or 3P BRCA1 folded into an alpha helix, we would expect to see the BRCA1+PALB2 curves (black and orange respectively) take on the same characteristically alpha helical shape of PALB2 alone (purple cure). Since we do not see this result and yet we see binding with NMR, the heptad coiled-coil predictive interface shown in **Figure 2** would not be useful for predicting which variants of unknown significance affect the BRCA1-PALB2 binding interface. Thus, we switched our focus from making a predictive model to developing a method that can be used to measure binding between constructs quantitatively to develop a system in which to test variants of unknown significance.

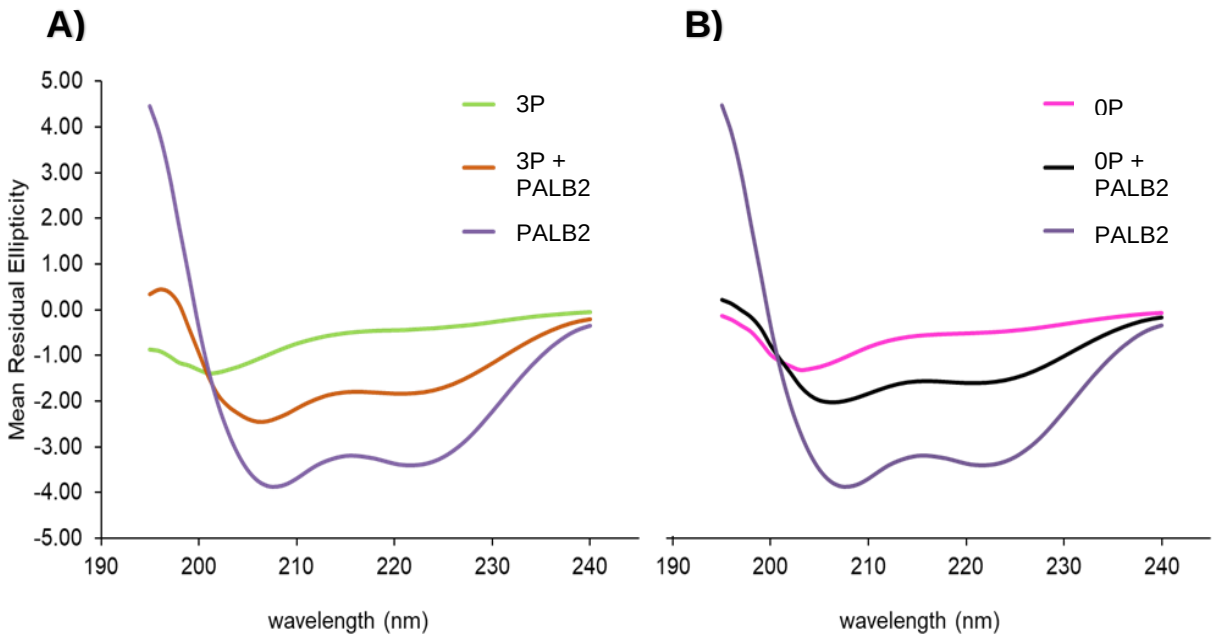

Figure 4) BRCA1 remains intrinsically disordered in the presence of a PALB2 construct. A) 3P BRCA1 is largely disordered even when added in a 1:1 ratio with PALB2 1-93, which is characteristically alpha helical. B) This CD curve has an exactly similar trend for 0P BRCA1. If there were folding upon binding, then the combination of the two proteins would resemble the PALB2 alone curve. (Reproduced with modification from Brian Morote-Costas Honor's Thesis).

Phosphomimetic constructs of PALB2 do not behave differently from a construct without phosphorylative control

In attempting to discern the best model to test the disruption of the BRCA1-PALB2 interface, we wanted to measure if the addition of the activating phosphomimetic construct (PALB2 1-93 S59E) or the inactivating phosphomimetic construct (PALB2 1-93 S64E) changed the nature of the binding interface by observing the BRCA1 side of the interaction. In the experiments in **Figure 5**, amino acids in our protein construct of BRCA1 that were isotopically labelled with $_{15}$N

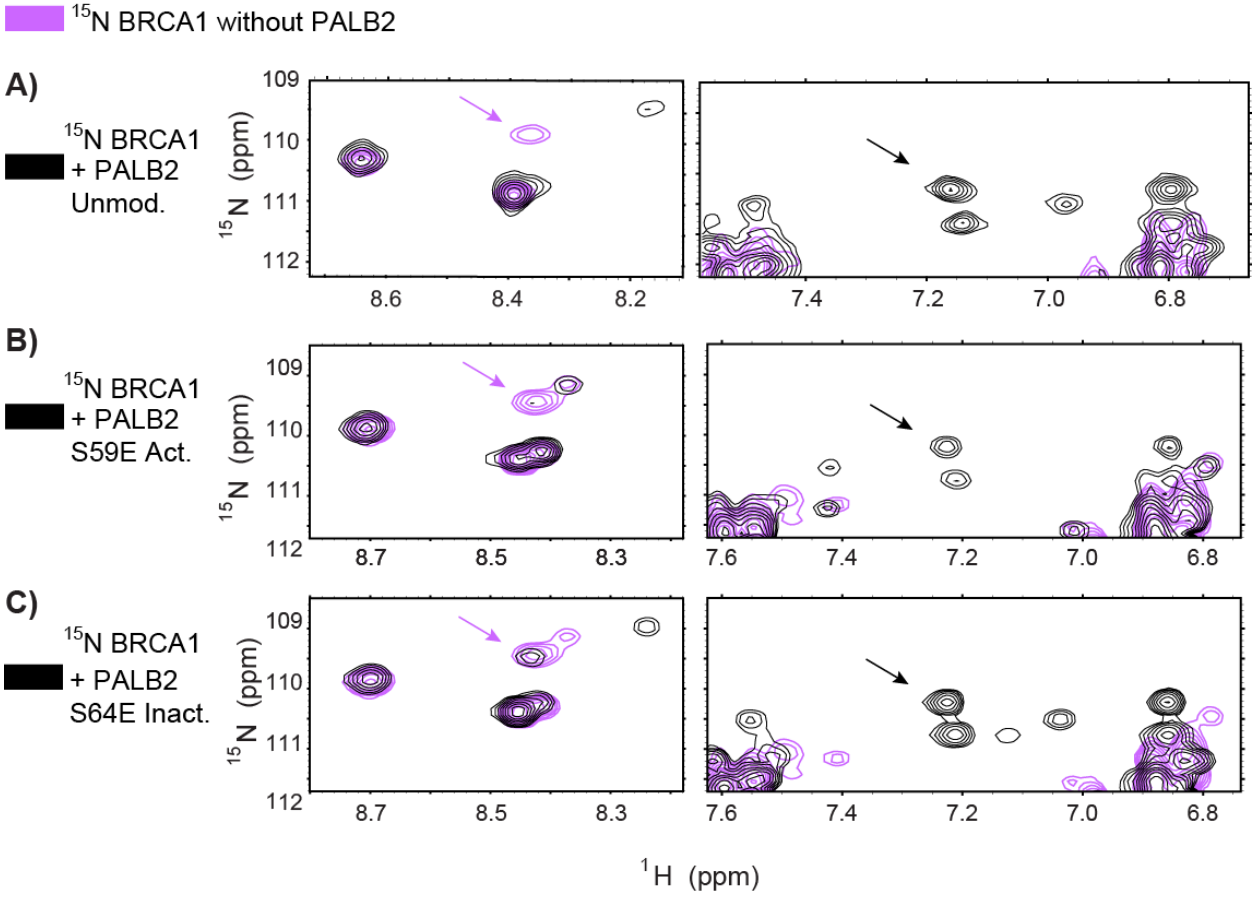

Figure 5) All three PALB2 constructs bind to BRCA1 and phosphomimetic PALB2 constructs using the same interface. Isotopically labeled 0P BRCA1 1377-1467 is represented by purple. For all three images, PALB2 constructs were then titrated in to arrive at a 1:1 ratio. A) 0P BRCA1 1377-1467 titrated with PALB2 1-56. B) 0P BRCA1 1377-1467 titrated with PALB2 1-93 S59E activating phosphomutant. C) 0P BRCA1 1377-1467 titrated with PALB2 1-93 S64E inactivating phosphomutant.

are represented by the lavender peaks. The black peaks correspond to the chemical environment of BRCA1 residues when the various PALB2 constructs are added. Comparison of black spectra in **5A** versus **5B** versus **5C** reveals that while the strength of the peaks differ depending on which PALB2 construct is added, the chemical shift locations are similar. Thus, we have concluded that there is no discernible difference in the binding interface between the three PALB2 constructs; instead, the strength of peaks changing represents a change in affinity. If we had observed folding upon binding—indicated by a spread in the range of the chemical shifts—in one of the constructs (most likely the activating phosphomimetic), then that would have been evidence for a conformational change being triggered by that specific phosphorylation event.

Developing an *in vitro* method using isothermal titration calorimetry to measure the effects of deleterious mutations in a disordered BRCA1-PALB2 binding interface

Given that we could not predict mutations in the BRCA1-PALB2 binding interface using the heptad coiled-coil structure, we needed a method that could be used to assess qualitative binding interface changes with the ultimate goal of assessing the magnitude of changes quantitatively. Isothermal titration calorimetry (ITC) is a method used to measure the enthalpic component of a chemical interaction. In addition to being a useful tool to assess drug affinity or reactions between small molecules, it can also be used to assess binding between two protein constructs if the concentration is known. [22] When creating an *in vitro* method to measure if a variant of BRCA1 or PALB2 maintain binding interaction, ITC experiments have the advantages of being quantitative, inexpensive, and several can be conducted in one day. For each experiment, the ITC machine uses a syringe to deliver small injections of one protein into a temperature-controlled cell containing another protein. As the syringe protein is titrated into the cell protein, the machine records exactly how much power it is delivering to the cell in order to keep it at a

constant temperature. If a binding event is exothermic, then the raw thermal data will show a series of steep dips, as the machine must provide less power since the reaction is providing heat to the system; the reverse is true for an endothermic binding event, characterized by a series of steep positive peaks. To develop our method, we need to determine which of our constructs provides the best ITC profile for testing binding disruption. First, we assessed the difference between 0P and 3P BRCA1 constructs when titrated into the same PALB2 construct (**Figure 6**).

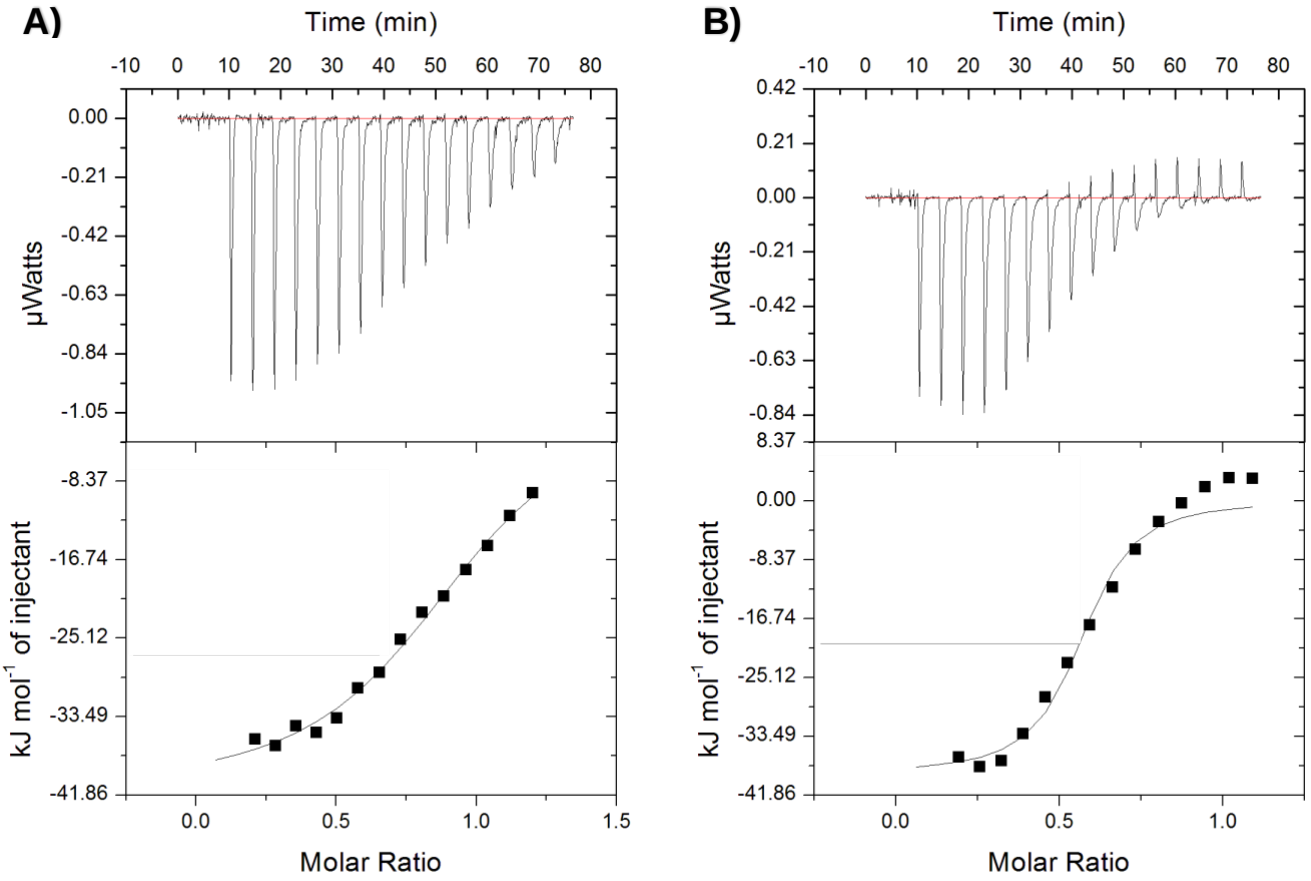

Figure 6: Both 3P and 0P BRCA1 constructs bind to PALB2 1-56 with high affinity. A) Top graph depicts the change in energy input needed to maintain a constant temperature for 3P BRCA1 titrated into a cell containing 60 µM of PALB2 1-56. Each spike represents a titration of 2µl of BRCA1. Bottom graph depicts the change in heat for the corresponding energy changes at as a function of the ratio of BRCA1 to PALB2. B) Top graph depicts the raw data for 0P BRCA1 titrated into a cell containing 66 µM of PALB2 1-56. Bottom graph depicts ΔH for the corresponding raw data above. K_d information for both curves is provided in Supplemental Table 1.

We found that we could observe binding to PALB2 1-56 in both constructs; however, 3P BRCA1 provided an advantage of being a completely exothermic interaction. In the 0P BRCA1+ PALB2 1-56 experiment, we can see that there is an endothermic component of the interaction that happens as PALB2 1-56 becomes saturated, which means there is potentially an extra binding or disassociation event that makes it more difficult to fit the binding disassociation curve. Since our goal is to eventually quantify to what magnitude a given patient VUS might disrupt the binding interface, having a control curve that only has one dimension is attractive. Since 3P BRCA1 has three negatively charged glutamate residues that are capable of forming ionic salt bridges, we believe this is responsible for the increase in the exothermic signal.

Consistent with NMR experiments, PALB2 phosphomimetic constructs behave similarly to PALB2 1-56 in ITC experiments

In order to see if phosphorylation has an effect on the PALB2 side of the interface that was measurable by ITC, we performed similar ITC experiments to those described above (**Figure 7**). Preliminary K_d data, which is reported in Supplemental Table 1, shows that the PALB2 1-56 experiments demonstrate the highest affinity with the most reliable statistical fit. Compared to the PALB2 1-93 constructs, PALB2 1-56 is also a well-behaved, easily purifiable protein; for the S59E experiments, completely purifying the construct from its SUMO solubility tag proved difficult—especially because gel filtration is not an attractive option given the similar molecular weights of the solubility tag and the construct. Of note is the result that PALB2 1-93 S64E did not abolish binding to BRCA1, implying that its method of control is not through direct modulation of the BRCA1-PALB2 interface. However, because all constructs have been shown to bind, the longer 1-93 PALB2 constructs could be useful for testing VUS in PALB2 amino acids between 56 and 93.

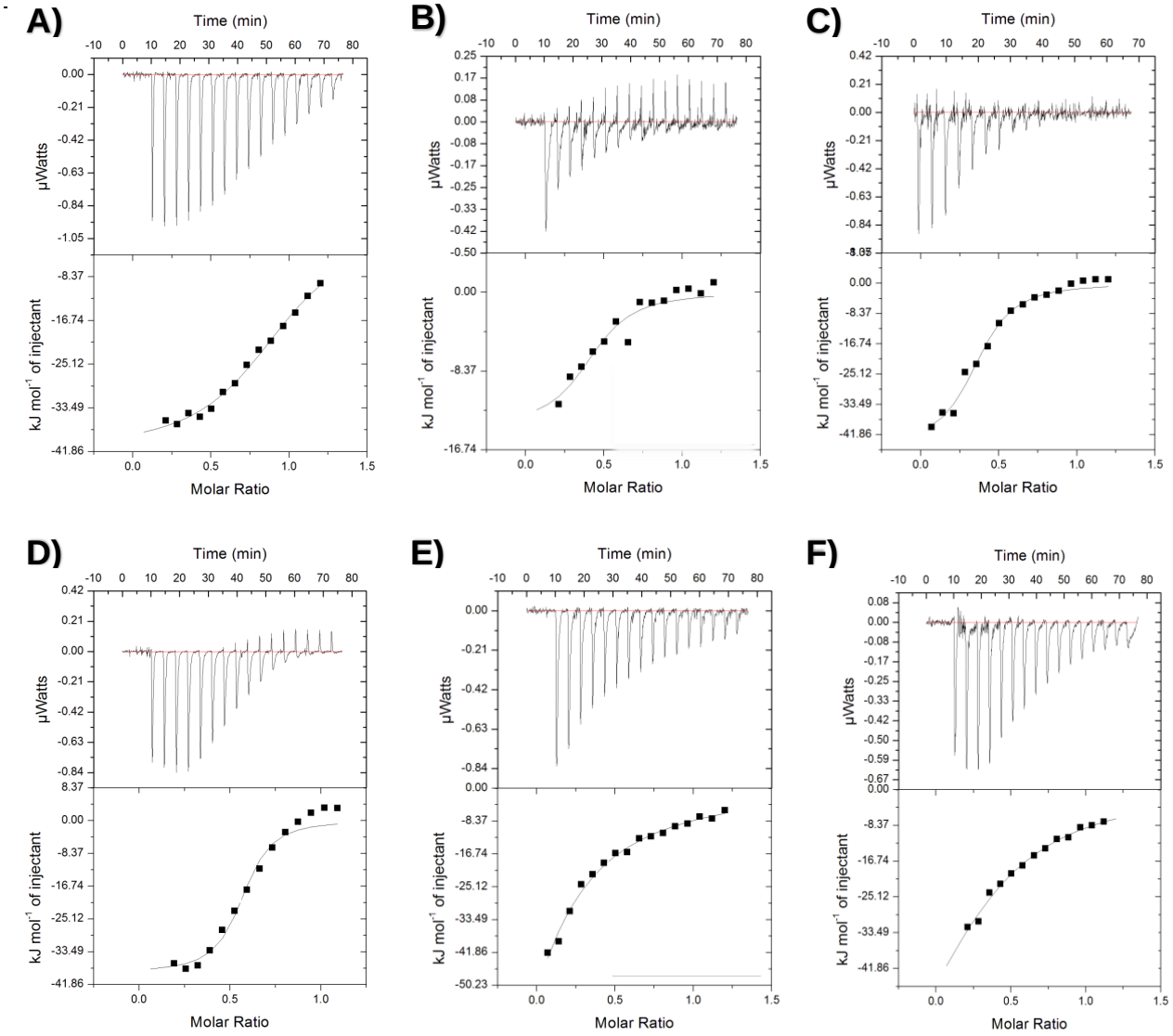

Figure 7) All phosphorylative states of PALB2 and BRCA1 exhibit binding in ITC. A) 425 μM 3P BRCA1 titrated into 60 μM PALB2 1-56, also represented in Figure 5a. B) 425 μM 3P BRCA1 titrated into "60" μM PALB2 1-93 S59E. C) 425 μM 3P BRCA1 titrated into 60 μM PALB2 1-93 PALB2 S64E. D) 425 μM 0P BRCA1 titrated into 66 μM PALB2 1-56, also represented in Figure 5b. E) 425 μM 0P BRCA1 titrated into 60 μM PALB2 1-93 S59E activ. F) 425 μM 0P BRCA1 titrated into 60 μM PALB2 1-93 S64E deact. ITC experimental specifications are reported in the methods section and K_d data is reported in Supplemental Table 1.

Using our *in vitro* model of the BRCA1-PALB2 interface, we were able to demonstrate a disruption of binding using a likely deleterious mutation, PALB2 L35P

Our NMR, CD, and ITC results describe different facets of the same binding event. However, while different phosphorylation states of BRCA1 and PALB2 result in different binding affinities, the binding interface remains the same even if the enthalpic profile changes. Since our data does not support the predictive model of the heptad coiled-coil, an ITC model was most appropriate to test deleterious mutations. For the reasons enumerated in the previous two sections, we determined that 3P BRCA1 and truncated PALB2 1-56 represents the clearest signal we can use to test the potential binding interruption of patient Variants of Unknown Significance. To test this model, we compared our exothermic BRCA1 3P + PALB2 1-56 data to BRCA1 3P titrated into the same construct that had been mutated using site-directed mutagenesis to include an L35P mutation. L35P is a known deleterious mutation that affects BRCA1 binding. **In Figure 8**, we show that while the positive control experiment of 3P BRCA1 titrated into PALB2 1-56 resulted in the characteristically exothermic profile of that interface, a second experiment that titrated 3P into a cell containing PALB2 1-56 L35P resulted in a loss of binding, demonstrated by the loss of signal. This result is vital as not only a proof of concept, but it also provides a negative control for comparing its abolition of binding to other patient VUS in this interface.

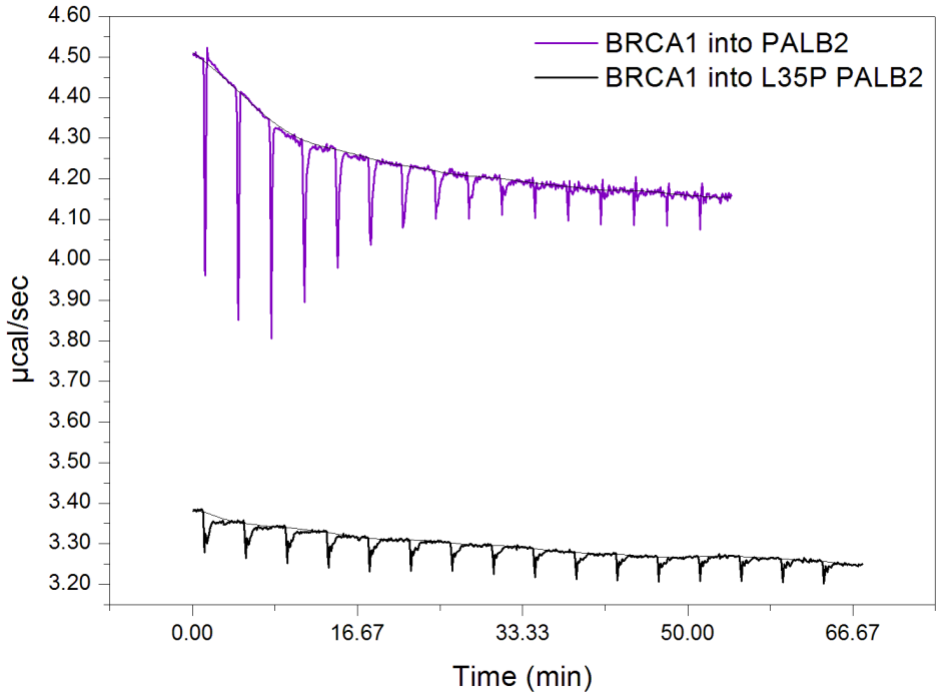

Figure 8) L35P PALB2 construct abolishes binding in an *in vitro* ITC model Shown above is the raw ITC data for 425 µM 3P BRCA1 being titrated into 60 µM PALB2 1-56 (purple) in one experiment and 425 µM 3P BRCA1 being titrated into 60 µM PALB2 1-56 L35P (black). ITC parameters for this experiment are detailed in the Methods Section.

III.DISCUSSION

The structural insights into the BRCA1-PALB2 interface

In terms of the structural insights that we have gained into the BRCA1-PALB2 interface, it is notable that we have demonstrated through our NMR experiments in Figures 3 and 5 that BRCA1 does not need to fold into an alpha helix in order to bind to PALB2. This is a piece of evidence that argues for a phenomenon present among many intrinsically disordered regions (IDR) and intrinsically disordered proteins (IDP) called "fuzzy complexes." [23] In a fuzzy complex, instead of forming one well-defined structure upon binding to another protein or nucleotide, an IDR instead forms multiple loose associations with its binding partner to bring about an overall high affinity. Examples of IDRs interacting while remaining unfolded include domains in the measles virus proteins. [24] Not unlike BRCA1, IDRs are also frequently associated with phosphorylation sites, which are interspersed among disorder-promoting residues with high frequency. [25] Many cancer-associated proteins have intrinsically-disordered regions and gain advantages from this disorder, including the favorability of interaction with a greater array of binding partners, an advantage to proteins in complexes like BRCA1. [26] Therefore, a world in which BRCA1 does not fold into the previously predicted alpha helix as it is observed in our experiments is consistent with similar systems in the literature. The data presented here was collected using truncated BRCA1 and PALB2 constructs so we cannot rule out that the full length proteins may assist BRCA1 with folding into an alpha helix upon interaction with PALB2; however, because we observed specificity of binding and high affinity interactions we conclude this structural transition is not a requirement.

Our findings that the phosphomimetic mutations did not induce large structural changes, but instead had modest effects on binding affinity is consistent with other systems described in

the literature. The effects of phosphorylation on secondary structure and ligand affinity can vary tremendously even within the same protein. For example, phosphorylation of one serine in calmodulin increases alpha helix formation, while phosphorylation at another serine four residues away decreases alpha helix formation. [27] As is summarized neatly in a review article of the effects of phosphorylation, it can 1) change structure to become more disordered or ordered, 2) reduce affinity for an anionic substrate, 3) induce a conformational change, 4) reduce protein-protein interactions, or 5) be silent. [28] There is also a possibility that even though this has worked in other *in vitro* systems, our phosphomimetic mutations did not accurately mimic the effect of phosphorylation on BRCA1 or PALB2 in the cell. [21] This could be tested by engineering the phosphomimetics into cells to observe their behavior with and without DNA damage. If we had observed significant structural or functional changes in the phosphomimetic constructs this would have been the next step to confirm the findings *in vivo*.

A cell-free assay to measure BRCA1 and PALB2 function

In **Table 2** we have listed several of the major benefits and drawbacks of our assay:

Table 2: Pros and cons of our cell-free assay

Pros	Cons
• Once system is calibrated, the limiting factor is speed of mutagenesis • Proteins can be purified in less than a week • ITC is sensitive, quantitative, and fast • Results are reproducible	• Mutations may affect purification protocol • ITC machinery can be overly sensitive to slight changes in buffer. Runs need to be consistent and controls performed often. • No information gained on DNA repair function or localization that cell assays provide

Table 2 (cont.)	
• Could be modified easily to measure other intrinsically disordered binding interfaces • More likely to identify detrimental mutations that cause moderate decreases in affinity	• Concentration of IDR can be challenging to assess which impacts reliably of binding constants • Intrinsically disordered proteins have a short shelf life outside of the freezer

The pros of our cell-free assay center mainly on the timeliness within which these experiments can be performed. For a given patient VUS, it could theoretically take as little as two weeks to move from first identifying the variant to an ITC final experimental result. In our experience calibrating mutagenesis annealing temperatures, confirming sequences, and troubleshooting protein purification parameters can extend this Platonic ideal into a longer timeframe, but in all of the patient VUS mutagenesis projects that have occurred in our lab, we have successfully created most of the mutant constructs with relative ease. In terms of minimizing the major cons of this assay, we have investigated and incorporated several strategies. We recently performed non-analytical gel filtration chromatography on BRCA1 which will allow more precise determination of the protein concentration by removing any higher absorbing impurities. In order to amplify the A_{280} signal, we are also considering adding a fluorophore onto our construct; however, since our interface is mostly a hydrophobic binding interface, we are concerned the hydrophobic fluorophore may change the binding affinities. In order to minimize the effect of proteolysis on BRCA1, we have used one protein prep and aliquoted samples that are removed from a -80°C freezer right before performing a given experiment. Troubleshooting the ITC machine was the main challenge of this project, but reproducible results were obtained after using and cleaning the machine consistently and conducting control experiments before and after

each run. Once these technical issues were solved, the experiments proceeded quickly and several could be conducted in one day.

The major requirement of this assay is incorporating patient VUS into the expression constructs. At time of publication, our lab has 13 patient VUS constructs ready to be tested on both sides of the interface using the cell-free assay. Once cell-free assays are applied to the VUS constructs and K_d information is obtained, then we would continue to draw from patient VUS databases for future studies; compared to a saturation method, this is a minor disadvantage to our assay as we cannot test every possible variant simultaneously. The function of some of these 13 VUS have been tested using cell-based assays, so our binding results will be compared with the ability of these mutants to perform DNA damage repair. We anticipate the cell-free assay will be more sensitive and provide more concise quantification of defects, but if this is not the case we would not continue to pursue a binding-based cell-free assay. As with any predictive method used, patient care decisions are best made when taking into account results from more than one type of assay. The desire is that the cell-free assay would provide easily obtainable complementary data for assessing patient risk.

IV.METHODS

Cloning

PALB2 full length human DNA was obtained from DNASU: Clone number: HsCD00295959.

BRCA1 full length human DNA was obtained from the Rachel Klevit Lab.

Table 3: Unmutated Construct Cloning Information			
Construct	**Direction**	**Annealing Temp**	**Primer Sequence**
BRCA1 1377-1467	Forward	58	5’ CGAT **GGATCC** AGC GTC TCT GAA GAC TGC TC 3’
	Reverse		5’ ATCG *GTCGAC* TTA CTG GCT TAT AGG GTA TTC ACTAC 3’
BRCA1 1362-1481	Forward	63	5’ CGAT **GGATCC** GAT TCA AAC TTA GGT GAA GCA GC 3’
	Reverse		5’ ATCG *GTCGAC* TTA TGC AGA CAC CTC AAA CTT GTC 3’
PALB2 1-56	Forward	55	5’ CGAT **GGATCC** ATG GAC GAG CCT CCCGG 3’
	Reverse		5’ ATCG *GTCGAC* TTA ATC TTG TTC TTC TAC TGT TTT CTT AAT AGA 3’
PALB2 1-93	Forward	55	5’ CGAT **GGATCC** ATG GAC GAG CCT CCC GG 3’
	Reverse		5’ ATCG *GTCGAC* TTA TCC AGT TTC TTC ATC AAG ATG GGT TTTGA 3’

Table 3: Unmutated Construct Cloning Information. Melting temperatures and primer sequences for full-length PALB2 and BRCA1 constructs. Purple text indicates non-specific flanker sequence, bolded text shows a BamHI restriction enzyme cut site, italicized text indicates a SalI restriction enzyme cut site, and red text indicates a stop codon.

Using the above primers, the PALB2 DNA regions of interest were amplified using PCR with New England BioLabs Q5 hot start high-fidelity Polymerase according to its protocol. Successful PCR was confirmed with DNA gel electrophoresis (1.5% agarose gel and Quick Load 1kb DNA ladder from NE BioLabs). DNA regions of interest and the pET SUMO plasmid were then separately digested with restriction enzymes BamHI and SalI (37°C, 1 hour). The cleaved products were separated by DNA gel electrophoresis, the bands were cut out, and DNA was separated from the gel using centrifugation (3000 rpm) through cotton. Ligation was then performed using DNA Ligase (NE BioLabs) according to corresponding protocol. 5 uL of ligated plasmid was transformed into 50 μL of DH5-α *E. coli* competent cell line and placed on ice for 25 minutes, heat shocked for 30 seconds at 42°C, iced for five minutes, and then incubated with 900 μL of SOC broth (Luria-Bertani + 20% glucose) for one hour in a shaker at 37°C. SOC/cell solution was centrifuged for 3 minutes at 3000 rpm, 700 μL of supernatant drawn off, and ~250 μL was resuspended and plated onto LB agar plates with 10ug/mL Kanamycin. After overnight (14-16 hours) incubation at 37°C, one colony was picked and placed in LB broth with corresponding antibiotic and grown overnight (14-16 hours) at 37°C in a shaker. The next morning, the cultures were spun down (3000 rpm, 4°C, 10 minutes) and the pellets were kept for DNA purification. DNA purification was accomplished by using a QIAgen mini-prep kit and performed according to protocol. Concentrations were confirmed using a Nano-Drop spectrophotometer, successful insertion was confirmed using PCR with the cloning primers and 1.5% agarose gel to observe the correct band length, and adherence was tested by sequencing as according to procedure described in the "Sequencing" methods section.

Growing/Purification for naturally abundant constructs

After being plated overnight from a glycerol stock or freshly transformed as described above in the Cloning section, constructs were grown in BL21-DE3 cells until OD_{600} 0.6 was reached. To induce protein expression, 0.25 mM of IPTG was added and cells were grown for 4 more hours at 37°C. Cells were spun down at 5000 rpm at 4°C for 25 minutes, resuspended in nickel column binding buffer, and either directly sonicated or frozen at -80°C for use at a later date. To lyse the cells, sonication took place on ice at 60 MHz on 85% amplification in 10 second pulses with 20 seconds of rest between pulses for a total pulse time of 10 minutes. Protease inhibitor, egg-white lysozyme, and DNAse were added before sonication. For BRCA1 constructs, a saturated solution of PMSF in 100% ethanol was added three times in 50 μL portions before, during, and after sonication in order to prevent protein degradation. Lysed cells were then spun down at 14000 rpm for 25 minutes at 4°C and purified using a Talon Crude cobalt column on an Äkta Start GE system. UV absorbance was measured and fractions were confirmed to contain proteins of interest using a 15% SDS PAGE gel. Fractions of interest were dialyzed overnight in a buffer containing 25 mM sodium phosphate, 150 mM NaCl, 1 mM DTT at pH 7. The SUMO tag was then cleaved off of the constructs using 200 ng of H3C protease by incubating at room temperature for one hour. Protein solution was then run through a GST column to remove GST-tagged H3C protease and then a nickel resin column to remove the His-tagged SUMO. The resultant protein of interest was usually in the flow-through or 30 mM imidazole eluted fraction and the location was confirmed with a 15% SDS PAGE Gel. Proteins were then dialyzed again overnight in 4L of 25 mM sodium phosphate buffer system, 50 mM NaCl with pH at 6.5. Proteins were concentrated and the A_{280} was measured on a Nano-Drop spectrophotometer or Pierce's BCA Assay as described in their protocol, and the concentration was calculated using

the estimated extinction coefficient as calculated by Expasy. Extinction coefficients are listed in Table EC below. Proteins were then stored long term in a -80°C freezer or kept at 4°C for a week or less before conducting experiments.

Table 4: Extinction Coefficients for Constructs Used

Construct Length	Constructs of this length	Extinction Coefficient
PALB2 1-56	PALB2 1-56, PALB2 1-56 L35P	1490
PALB2 1-93	PALB2 1-93, PALB2 1-93 S59E activ., PALB2 1-93 S64E deactiv.	2980
BRCA1 1377-1467	BRCA1 0P, BRCA1 3P	2980
BRCA1 1362-1481	BRCA1 0P LONG	2980

Circular Dichroism (CD)

The CD data in **Figure 5** was collected on a JASCO Corp., J-810 from 195-240nm. Concentrations were measured both by spectrometry and by a BCA assay. All samples were in 10mM HEPES, pH 7.4. Values were corrected for concentration and number of amino acids by using the following equation:

$$(MRE) = CD\ output / [\ d * (N-1) * M\ ]$$

Where MRE is the mean residual ellipticity, CD output is the value given by the instrument, d is the molar concentration, N is the number of amino acids in the construct, and M is the molecular weight of the protein in daltons.

Isothermal titration calorimetry

Isothermal calorimetry was used to measure the raw enthalpic data between PALB2 and BRCA1 constructs as reported in Figures 5, 6, and 7. All experiments were performed on a Malvern Microcal ITC$_{200}$ according to their instruction with a syringe rotation of 300 rpm and at 25°C. Samples with an initial delay of 600 seconds were brought to room temperature and spun down at 10,000 rpm for 5 minutes at 4°C before being allowed to return to room temperature. Specifications for each experiment are detailed in **Table 5** below. For the experiment in Figure 5B, "100 μM" of PALB2 1-93 S59E act. was used due to purification issues and an estimation of 60% purity based on an SDS-PAGE gel. ITC experiments were conducted in 50 mM NaCl and 25mM sodium phosphate buffer system at pH 6.5. All curves were fit using a single-site binding equation detailed in the Microcal ITC200 System User Manual (page 311-312). [29]

Table 5: ITC Machine parameters used for experiments displayed in Figures 5-7

Figure Number	Syringe Protein, Concentration (μM)	Cell Protein, Concentration (μM)	Injection #	Injection Volume (μL)	Spacing between injections (sec)	Stirring speed (rpm)	Initial Delay (sec)
5A, 6A	425 μM 3P BRCA1	PALB2 1-56, 60 μM	16	2	250	300	600
5B, 6D	0P BRCA1, 425 μM	PALB2 1-56, 66 μM	16	2	250	300	600
6B	3P BRCA1, 425 μM	PALB2 1-93 S59E act. ~ 60μM	16	2	250	300	600
6C	3P BRCA1, 425 μM	PALB2 1-93 S64E deact., 60 μM	16	2	250	300	60
6E	0P BRCA1, 425 μM	PALB2 1-93 S59E act. ~ 60μM	16	2	250	300	600

Table 5 (cont.)							
6F	0P BRCA1, 425 μM	PALB2 1-93 S64E deact., 60 μM	16	2	250	300	600
7 (purple)	3P BRCA1, 425 μM	PALB2 1-56, 60 μM	16	2	250	300	60
7 (black)	3P BRCA1, 425 μM	PALB2 1-56, L35P-del., 60 μM	16	2	250	300	60

Mutagenesis

A modified QuikChange protocol was used where the forward primer and reverse primer underwent PCR in separate reactions and then the products were annealed together before digestion. Site-directed mutagenesis for the 3P construct was performed according to specifications in Brian Morote-Costas's honors thesis 2019. Primers for each mutation were designed using protocol described in Edelheit et. al. [30]

Table 6: Mutagenesis Primers used for PALB2 phosphomimetics and L35P mutant		
Construct	**Direction**	**Primer Sequence**
PALB2 1-56 L35P	Forward	5' GACACTAGCCCGCCCGCAGCGTGCCCAAAG 3'
	Reverse	5' CTTTGGGCACGCTGCGGGCGGGCTAGTGTC 3'
PALB2 S59E	Forward	5' GAAGAACAAGATTGTTTGGAACAGCAGGATCTCTCACCG 3'
	Reverse	5' CGGTGAGAGATCCTGCTGTTCCAAACAATCTTGTTCTTC 3'
PALB2 S64E	Forward	5' GTCTCAGCAGGATCTCGAACCGCAGCTAAAACAC 3'
	Reverse	5' GTGTTTTAGCTGCGGTTCGAGATCCTGCTGAGAC 3'

Sequencing

To confirm successful mutagenesis for PALB2 and BRCA1 constructs sequencing was performed using a Hitachi Genetic Analyzer 3130XL according to the protocol outlined in ThermoFisher BigDye Terminator v3.1 Cycle Sequencing Kit. Sequence ends were trimmed with Sequencher and sequences were confirmed to be successfully mutated using Expasy.

Nuclear Magnetic Resonance

Proteins were isotopically labeled with ^{15}N according to protocol detailed in Marley et. al 2001. [31] All NMR experiments presented are ^{1}H-^{15}N heteronuclear single quantum coherence (HSQC) experiments. The experiments in Figure 2 as well as the unbound BRCA1 spectrum in Figure 4 were collected at Texas A&M University on a 500MHz magnet with a room temperature probe using standard Bruker pulse programs at 20°C. In Figure 4, titrations with PALB2 phosphomutants were performed at University of Washington on a 600MHz magnet with a cryoprobe using standard Bruker pulse programs at 20°C. All NMR spectra were collected in a sodium phosphate buffer system at pH 6.5 (25mM $NaPO_4$, 50mM NaCl).

APPENDIX

Table 7: ITC K_d information obtained from ITC experiments in Figures 5-7

Figure Number	Syringe Protein, Concentration (μM)	Cell Protein, Concentration (μM)	K_d (M^{-1})	N (sites)
5A, 6A	3P BRCA1, 425 μM	PALB2 1-56, 60 μM	$2.35 \times 10^{-5} \pm 3.36 \times 10^{-4}$	0.936 ± 0.0122
5B, 6D	0P BRCA1, 425 μM	PALB2 1-56, 66 μM	$1.31 \times 10^{-6} \pm 5.10 \times 10^{-5}$	0.552 ± 0.0168
6B	3P BRCA1, 425 μM	PALB2 1-93 S59E act. ~ 60μM	$3.40 \times 10^{-5} \pm 2.13 \times 10^{-5}$	0.427 ± 0.0609
6C	3P BRCA1, 425 μM	PALB2 1-93 S64E deact., 60 μM	$3.84 \times 10^{-5} \pm 9.48 \times 10^{-4}$	0.364 ± 0.0162
6E	0P BRCA1, 425 μM	PALB2 1-93 S59E act. ~ 60μM	$2.48 \times 10^{-4} \pm 6.28 \times 10^{-3}$	0.0768 ± 0.128
6F	0P BRCA1, 425 μM	PALB2 1-93 S64E deact., 60 μM	$3.99 \times 10^{-4} \pm 1.06 \times 10^{-4}$	0.372 ± 0.104

REFERENCES

1. Sy, S.M.H., M.S.Y. Huen, and J.J. Chen, *PALB2 is an integral component of the BRCA complex required for homologous recombination repair.* Proceedings of the National Academy of Sciences of the United States of America, 2009. **106**(17): p. 7155-7160.
2. Siegel, R.L., K.D. Miller, and A. Jemal, *Cancer statistics, 2020.* CA: A Cancer Journal for Clinicians, 2020. **70**(1): p. 7-30.
3. Couch, F.J., et al., *BRCA1 mutations in women attending clinics that evaluate the risk of breast cancer.* New England Journal of Medicine, 1997. **336**(20): p. 1409-1415.
4. Ford, D., et al., *Risks of cancer in BRCA1-mutation carriers.* The Lancet, 1994. **343**(8899): p. 692-695.
5. Hartmann, L.C. and N.M. Lindor, *The role of risk-reducing surgery in hereditary breast and ovarian cancer.* New England Journal of Medicine, 2016. **374**(5): p. 454-468.
6. Zhang, F., et al., *PALB2 Links BRCA1 and BRCA2 in the DNA-Damage Response.* Current Biology, 2009. **19**(6): p. 524-529.
7. Song, F., et al., *Antiparallel Coiled-Coil interactions mediate the homodimerization of the DNA Damage-Repair protein PALB2.* Biochemistry, 2018. **57**(47): p. 6581-6591.
8. Mark, W.Y., et al., *Characterization of segments from the central region of BRCA1: An intrinsically disordered scaffold for multiple protein-protein and protein-DNA interactions?* Journal of Molecular Biology, 2005. **345**(2): p. 275-287.
9. Xia, B., et al., *Control of BRCA2 cellular and clinical functions by a nuclear partner, PALB2.* Molecular Cell, 2006. **22**(6): p. 719-729.
10. Rahman, N., et al., *PALB2, which encodes a BRCA2-interacting protein, is a breast cancer susceptibility gene.* Nature Genetics, 2007. **39**(2): p. 165-167.
11. Easton, D.F. and R.A. Eeles, *Genome-wide association studies in cancer.* Human Molecular Genetics, 2008. **17**: p. R109-R115.
12. Chen, P., et al., *Association of common PALB2 polymorphisms with breast cancer risk: a case-control study.* Clinical Cancer Research, 2008. **14**(18): p. 5931-5937.
13. Han, M.-R., et al., *Evaluating genetic variants associated with breast cancer risk in high and moderate-penetrance genes in Asians.* Carcinogenesis, 2017. **38**(5): p. 511-518.
14. Foo, T.K., et al., *Compromised BRCA1-PALB2 interaction is associated with breast cancer risk.* Oncogene, 2017. **36**(29): p. 4161-4170.
15. Rodrigue, A., et al., *A global functional analysis of missense mutations reveals two major hotspots in the PALB2 tumor suppressor.* Nucleic acids research, 2019. **47**(20): p. 10662-10677.
16. Findlay, G.M., et al., *Accurate classification of BRCA1 variants with saturation genome editing.* Nature, 2018. **562**(7726): p. 217-3,222A-222P.
17. Buisson, R., et al., *Coupling of homologous recombination and the checkpoint by ATR.* Molecular cell, 2017. **65**(2): p. 336-346.
18. Gatei, M., et al., *Role for ATM in DNA damage-induced phosphorylation of BRCA1.* Cancer research, 2000. **60**(12): p. 3299-3304.
19. Wang, A., et al., *A single N-terminal phosphomimic disrupts TDP-43 polymerization, phase separation, and RNA splicing.* The EMBO Journal, 2018. **37**(5): p. e97452.
20. Jean, A., A. Gutierrez-Hartmann, and D.L. Duval, *A Pit-1 Threonine 220 Phosphomimic Reduces Binding to Monomeric DNA Sites to Inhibit Ras and Estrogen Stimulation of the Prolactin Gene Promoter.* Molecular Endocrinology, 2010. **24**(1): p. 91-103.

21. Yadav, S., et al., *Phosphomimetic-mediated in vitro rescue of hypertrophic cardiomyopathy linked to R58Q mutation in myosin regulatory light chain.* The FEBS Journal, 2019. **286**(1): p. 151-168.
22. Pierce, M.M., C. Raman, and B.T. Nall, *Isothermal titration calorimetry of protein–protein interactions.* Methods, 1999. **19**(2): p. 213-221.
23. Tompa, P. and M. Fuxreiter, *Fuzzy complexes: polymorphism and structural disorder in protein-protein interactions.* Trends in Biochemical Sciences, 2008. **33**(1): p. 2-8.
24. Bourhis, J.M., et al., *The intrinsically disordered C-terminal domain of the measles virus nucleoprotein interacts with the C-terminal domain of the phosphoprotein via two distinct sites and remains predominantly unfolded.* Protein Science, 2005. **14**(8): p. 1975-1992.
25. Iakoucheva, L.M., et al., *The importance of intrinsic disorder for protein phosphorylation.* Nucleic Acids Research, 2004. **32**(3): p. 1037-1049.
26. Iakoucheva, L.M., et al., *Intrinsic disorder in cell-signaling and cancer-associated proteins.* Journal of Molecular Biology, 2002. **323**(3): p. 573-584.
27. Vetter, S.W. and E. Leclerc, *Phosphorylation of serine residues affects the conformation of the calmodulin binding domain of human protein 4.1.* Eur J Biochem, 2001. **268**(15): p. 4292-9.
28. L N Johnson, a. and D. Barford, *The Effects of Phosphorylation on the Structure and Function of Proteins.* Annual Review of Biophysics and Biomolecular Structure, 1993. **22**(1): p. 199-232.
29. Corporation, M. *ITC200 User Manual*. 2014; Available from: https://www.google.com/url?sa=t&rct=j&q=&esrc=s&source=web&cd=1&ved=2ahUKEwiE6oXA09ToAhUHR6wKHTNpD_YQFjAAegQIAhAB&url=http%3A%2F%2Fwww.isbg.fr%2FIMG%2Fpdf%2Fmicrocal-itc200-system-user-manual-malvern.pdf&usg=AOvVaw3sIa_7QK20tve_BwM43kN8.
30. Edelheit, O., A. Hanukoglu, and I. Hanukoglu, *Simple and efficient site-directed mutagenesis using two single-primer reactions in parallel to generate mutants for protein structure-function studies.* BMC biotechnology, 2009. **9**(1): p. 61.
31. Marley, J., M. Lu, and C. Bracken, *A method for efficient isotopic labeling of recombinant proteins.* Journal of biomolecular NMR, 2001. **20**(1): p. 71-75.

VITA

Christine Ann Hurd was born in Omaha, Nebraska on June 18th, 1991. She is the daughter of Doris and Kevin Hurd. She graduated from Aledo High School in 2009. She received her Artium Baccalaureus in Government with a foreign language citation in German from Harvard College in 2013. After working as a travel writer, she decided to complete her post-baccalaureate requirements for medical school at Texas Christian University. During her time there, she joined Dr. Mikaela Stewart's lab and began pursuing her Master of Science degree in Biology from Texas Christian University in 2018. She will be attending Texas College of Osteopathic Medicine in Fall 2020.

ABSTRACT

CREATING A CELL-FREE ASSAY
TO ASSESS THE BINDING AFFINITY
OF PATIENT VARIANTS IN THE
BRCA1-PALB2 INTERFACE

By Christine A. Hurd
Department of Biology
Texas Christian University

Mikaela D. Stewart, Assistant Professor of Biology

Giridhar R. Akkaraju, Professor of Biology and Chair of the Department

Meredith Curtis, Instructor of Biology

BRCA1 and PALB2 are two important proteins necessary for DNA repair of double-stranded breaks via homologous recombination. Defects in this repair mechanism can lead to genomic instability and a higher rate of mutation acquisition, leading to an increased risk of breast and ovarian cancer. Patient variants of unknown significance (VUS) located in the BRCA1-PALB2 binding interface are currently being studied using *in vivo* biochemistry methods in order to measure a loss of function or using segregation analysis. Along with gaining structural insights into this binding interface using nuclear magnetic resonance (NMR), we have developed an *in vitro*, cell-free assay to study the BRCA1-PALB2 binding interface using isothermal titration calorimetry (ITC). This assay will be used in future Stewart Lab research to assess changes in binding affinity of patient variants.